

On the Escape of a Resonantly Excited Couple of Colliding Particles from a Potential Well under Bi-harmonic Excitation

Attila Genda^{*}, Alexander Fidlin^{*} and Oleg Gendelman^{**}

^{*}*Institute of Engineering Mechanics, Karlsruhe Institute of Technology, Karlsruhe, Germany*

^{**}*Mechanical Engineering, Technion – Israel Institute of Technology, Haifa, Israel*

Summary. Escape dynamics of a damped two-particle system with internal collisions in a truncated quadratic potential well under biharmonic excitation is investigated. It is assumed that the excitation frequencies are tuned to the $2l$ -fold values of the modal natural frequency of the relative motion and to the modal frequency of the center of mass on the bottom of the potential well. Although the escape is an essentially non-stationary process, the critical forcing amplitude strongly depends on the stationary amplitudes of the relative vibrations within the two particles. The characteristic escape curve for the critical force moves up with the increasing relative vibrations.

Introduction

Escape from a potential well is an important topic in non-linear dynamics. The problem arises in various fields of physics and engineering [1]-[5].

A broad spectrum of physical phenomena from the dynamics of molecules to celestial mechanics has been studied in the literature, discussing topics such as energy harvesting [6], the physics of Josephson junctions [7], transient resonance dynamics of oscillatory systems [8, 9] or such phenomena as capsizing of ships [3, 10]. A further example for an escape related topic is the dynamic pull-in in microelectromechanical systems (MEMS) [11]-[16].

First, in 1940, Kramer started to investigate the forced escape phenomenon regarding the thermal activation of chemical reactions [17, 18]. Despite of much research which has taken place in the last 80 years, important unsolved problems still exist regarding the escape process [19].

In the case of constant forcing, escape might occur as a consequence of the slow variation of the system parameters which leads to subsequent bifurcations of the steady-state regimes of the response [2, 11, 12]. Thompson investigates extensively the mechanisms leading to escape in a cubic model potential. His numerical results describe the phenomenon of escape along a broad scale of the excitation frequency of the harmonic forcing. It reveals the chaotic processes leading to escape near the critical forcing amplitude curve. Using Melnikov's method [32] a good approximation can be given for the numerical location of a part of the critical force curve.

Different modeling approaches can be found in the literature to give analytic criteria for the escape. In the paper of Virgin, [3] harmonically forced and damped particles are investigated in three different model potentials, where the steady state response of the particle's motion is used to obtain the partly empirically corrected analytic criterion. The author assumes a harmonic response with an additional bias to correct asymmetries of the potential.

Technically relevant potential wells in general exhibit a monotonically decreasing stiffness when moving away from the center of the potential well. This is necessary to flatten out the profile of the potential, otherwise its depth could not be finite.

In the paper [3] some model potential wells are also investigated numerically. The numerical results show a sharp minimum of the critical forcing amplitude depicted along the forcing frequency. This sharp minimum takes smaller values than the linearized eigenfrequency of the potential well. Papers [14, 15] investigating the problem of dynamic pull-in in MEMS devices also come to similar results regarding the shape of the critical forcing curve.

In the papers [20, 21] investigating the safe basins of attraction for various dynamical systems similar patterns for the sharp minimum were found. This let's the reader formulate a hypothesis about the above mentioned feature of the critical forcing curve as an inherent property of the escape phenomena. In the papers [22, 25] for different potentials this hypothesis was investigated using harmonic forcing.

The above two papers investigate the escape dynamics of the harmonically forced bodies assuming 1:1 resonance. The applied method is able to take into account the transient dynamics of the system, which can be described by the slow flow on the resonance manifold. Varying the initial conditions (IC) allows the identification of two different escape mechanisms. The simpler to describe maximum mechanism (MM) corresponds to the case when the oscillation amplitude reaches the escape threshold as a consequence of the excitation. In this case, exciting with the critical force results in an amplitude value that just reaches the escape threshold. The other mechanism is the so called saddle mechanism (SM). It is different from the previous mechanism, because the amplitude of the vibration stays quite small even if the forcing amplitude is almost critical. When the critical forcing amplitude is reached, the vibration amplitude starts to increase abruptly and escape takes place. At the lowest point of the critical force curve both mechanisms can be observed at the same time. The approach resembles the research done in [23, 24] describing transient phenomena in coupled oscillator systems with the use of limiting phase trajectories (LPT).

In paper [28] a system of a pair of strongly coupled particles in a truncated quadratic potential well with a bi-harmonic excitation, consisting of a high and a low frequency component, was investigated. The paper introduced a new method to model the effect of the high-frequency excitation using an effective force field which was derived by convolution of the original force field and the probability density function of the fast movement around the center of mass of the two particles.

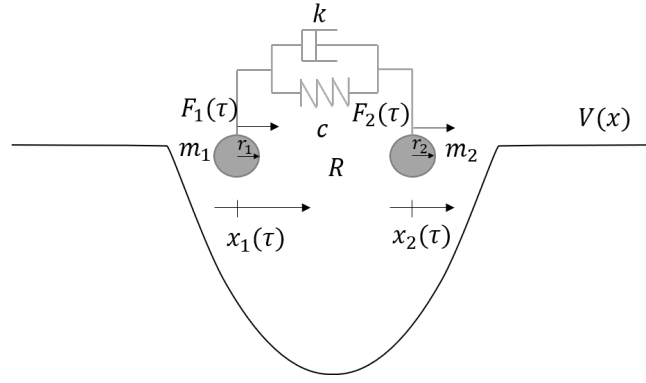


Figure 1: The setting of the collision problem in a potential well with harmonic force excitation.

The multi-body problem was simplified that way to a single body problem for which standard techniques could be applied. The research also showed that the high-frequency excitation has a stabilizing effect on the escape behavior with the used model potential, for which, being the model of a linear oscillator, a single particle has a critical forcing amplitude tending to 0 at the the resonance frequency. In the case of two bodies, however, the minimal value of the critical force curve is greater than 0 and it is shifted to a lower frequency than the linearized eigenfrequency of the potential.

In the present paper, the model presented in [28] is modified such that the particles, although they are still considered as point masses, are not able to penetrate each other, but an almost elastic collision, with the coefficient of restitution R takes place every time they get in touch with each other, i.e. the distance between them is $\Delta := r_1 + r_2$.

First, the mathematical model of the problem is introduced. Then, after bringing the equations into an appropriate form using a coordinate transformation, the first step of the model reduction based on the so called 'unfolding transformation' is described. With the use of this result, the further reduction of the model takes place in the next section, which is based on a probabilistic type of averaging, that leads to a single particle problem in a modified, effective potential. In the section 'Numerical results and discussion' the reduced model is compared to the original problem by direct numerical integration using parameter values spanned by a grid on the excitation frequency – force amplitude plane, highlighting the stabilizing effect of the high-frequency excitation. The findings of the paper are summarized in the 'Conclusions' section.

Description of the model

Let us consider the following problem setting depicted in Fig. 1.

The coupled pair of particles with masses m_1 and m_2 is excited harmonically in a one-dimensional quadratic potential well. The linear spring between the particles has the stiffness $k \gg 1$ and the linear damper is described by the damping coefficient c of $\mathcal{O}(1)$. The potential well is defined individually for both of the particles by $V_1(x) = m_1 V(x)$ and $V_2(x) = m_2 V(x)$, respectively, where m_1 and m_2 are of $\mathcal{O}(1)$. Poly-harmonic forces, given by $F_1(t)$ and $F_2(t)$, respectively, can act on both of the bodies. The particles cannot penetrate through each other and hence collide every time they are at a distance $\Delta := r_1 + r_2$ from each other. The collision is nearly elastic, which means the coefficient of restitution is close to one, i.e. $R \approx 1$.

The differential equations describing the motion of the system are given by

$$\begin{bmatrix} m_1 & 0 \\ 0 & m_2 \end{bmatrix} \begin{bmatrix} \ddot{x}_1 \\ \ddot{x}_2 \end{bmatrix} + \begin{bmatrix} c & -c \\ -c & c \end{bmatrix} \begin{bmatrix} \dot{x}_1 \\ \dot{x}_2 \end{bmatrix} + \begin{bmatrix} k & -k \\ -k & k \end{bmatrix} \begin{bmatrix} x_1 \\ x_2 \end{bmatrix} + \begin{bmatrix} m_1 V'(x_1) \\ m_2 V'(x_2) \end{bmatrix} = \begin{bmatrix} F_1(\tau) \\ F_2(\tau) \end{bmatrix} \quad \text{if } x_1 + \Delta < x_2, \quad (1)$$

$$x_{1+} = x_{1-}, \quad x_{2+} = x_{2-}, \quad \text{if } x_1 + \Delta = x_2, \quad (2)$$

$$\dot{x}_{1+} = \frac{Rm_2(\dot{x}_{2-} - \dot{x}_{1-}) + m_1\dot{x}_{1-} + m_2\dot{x}_{2-}}{m_1 + m_2}, \quad \dot{x}_{2+} = \frac{Rm_1(\dot{x}_{1-} - \dot{x}_{2-}) + m_1\dot{x}_{1-} + m_2\dot{x}_{2-}}{m_1 + m_2}, \quad (3)$$

where V is defined as

$$V(x) = \begin{cases} \frac{1}{2}x^2 - \frac{1}{2} & |x| \leq 1, \\ 0 & |x| > 1, \end{cases} \quad (4)$$

The excitation force can be chosen in general as

$$F_j(\tau) = \sum_{i=1}^p A_{ji} \sin(\Omega_{ji}\tau + \beta_{ji}), \quad \text{with } j \in 1, 2 \text{ and } p \in \mathbb{N}^+. \quad (5)$$

In order to be able to excite the center of the mass in the potential well and the relative vibrations within the particles simultaneously, the excitation in the current investigation is chosen to be

$$F_1(\tau) = F_{11} \sin(\Omega_{11}\tau + \beta_{11}) + F_{12} \sin(\Omega_{12}\tau + \beta_{12}), \quad (6)$$

$$F_2(\tau) = 0. \quad (7)$$

The coordinates x_1 and x_2 can be linearly transformed to the new coordinates

$$y_1 := \frac{m_1 x_1 + m_2 x_2}{m_1 + m_2}, \quad y_2 := x_2 - x_1, \quad (8)$$

thus, y_1 describes the movement of the particle's center of mass and y_2 gives the distance between the particles. By having collisions, y_2 can never be smaller than Δ . The inverse of the coordinate transformation is substituted back into Eq. (1), which leads to

$$\begin{aligned} \ddot{y}_1 + \mu V'(y_1 - (1 - \mu)y_2) + (1 - \mu)V'(y_1 + \mu y_2) \\ = \frac{1}{m_1 + m_2} (F_{11} \sin(\Omega_{11}\tau + \beta_{11}) + F_{12} \sin(\Omega_{12}\tau + \beta_{12})) \quad \text{if } y_2 > \Delta, \end{aligned} \quad (9)$$

$$y_{1+} = y_{1-}, \quad \dot{y}_{1+} = \dot{y}_{1-}, \quad \text{if } y_2 = \Delta, \quad (10)$$

$$\begin{aligned} \ddot{y}_2 + \frac{c}{m} \dot{y}_2 + \frac{k}{m} y_2 + \underbrace{V'(y_1 + \mu y_2) - V'(y_1 - (1 - \mu)y_2)}_{\text{small coupling term of } \mathcal{O}(1) \text{ since } \frac{k}{m} \gg V'(x)} \\ = -\frac{F_{11}}{m_1} \sin(\Omega_{11}\tau + \beta_{11}) - \frac{F_{12}}{m_1} \sin(\Omega_{12}\tau + \beta_{12}) \quad \text{if } y_2 > \Delta, \end{aligned} \quad (11)$$

$$y_{2+} = y_{2-}, \quad \dot{y}_{2+} = -R\dot{y}_{2-}, \quad \text{if } y_2 = \Delta, \quad (12)$$

with

$$\frac{1}{m} := \frac{1}{m_1} + \frac{1}{m_2}, \quad \mu := \frac{m_1}{m_1 + m_2}. \quad (13)$$

Eq. (11) is coupled to Eq. (9) only through a small term, which, if both terms of the sum are evaluated inside of the potential, is equal to y_2 and if both terms are evaluated outside of the potential, is equal to 0. Otherwise, the small coupling term is not independent of y_1 anymore, but still, even in this case the force of the potential is very small compared to the force of the spring. In addition, the case, when both particles are in the potential well, is the most dominant one, thus the small coupling term can be approximated by y_2 very well. By doing so, Eq. (11) becomes linear and can be solved easily.

$$\ddot{y}_2 + \frac{c}{m} \dot{y}_2 + \left(\frac{k}{m} + 1 \right) y_2 = -\frac{F_{11}}{m_1} \sin(\Omega_{11}\tau + \beta_{11}) - \frac{F_{12}}{m_1} \sin(\Omega_{12}\tau + \beta_{12}) \quad \text{if } y_2 > \Delta, \quad (14)$$

$$y_{2+} = y_{2-}, \quad \dot{y}_{2+} = R\dot{y}_{2-}, \quad \text{if } y_2 = \Delta, \quad (15)$$

Since the damping coefficient, $\frac{c}{m}$ in the investigated case is not small, the homogeneous solution will decay in relatively short time and the relevant part of the solution becomes the particular solution [29]-[30]. The frequency of the resonance peak in the motion of y_2 without collision would be

$$\Omega_{02} = \sqrt{\frac{k}{m} + 1 - \frac{c^2}{2m^2}}, \quad (16)$$

but the collisions have a significant effect on the high frequency vibration, which has to be discussed first in order to be able to determine the vibration amplitude and so the probability density function (PDF) of the high-frequency oscillations. In the current investigation we are interested in the escape behavior of the two-particle system with large inner vibrations under a low-frequency and small force amplitude excitation. To get large vibrations in the relative motion of the particles the appropriate excitation frequencies should be found.

The resonance frequency of the particle's center of mass in the potential well is not influenced by the collisions. When both particles are in the potential well, Eq. (9) simplifies to

$$\ddot{y}_1 + y_1 = \frac{1}{m_1 + m_2} (F_{11} \sin(\Omega_{11}\tau + \beta_{11}) + F_{12} \sin(\Omega_{12}\tau + \beta_{12})), \quad (17)$$

which means that the linearized eigenfrequency of y_1 is $\Omega_{01} = 1$.

In the next section the focus is set on the description of the vibration amplitude of the relative movement depending on the choice of the excitation frequency.

The first step of the model reduction: resonance of the colliding particles under high-frequency excitation

The analysis of the resonance frequencies of Eq. (14) is already performed by *Fidlin* in chapter 3.5 of [31]. In the present section of this paper the content of the book is repeated mostly, however, due to a printing error in the book, a somewhat different result is obtained in the end.

In order to be able to apply the results from the book, a preliminary step is needed. With a coordinate transformation it has to be ensured that the term y_2 in Eq. (14) has the coefficient 1.

Introducing the new, dimensionless time $t = \omega_0 \tau$, with $\omega_0 = \sqrt{\frac{k}{m} + 1}$ the time derivatives can be rewritten as follows

$$\dot{y}_2 = \frac{dy_2}{d\tau} = \omega_0 \frac{dy_2}{dt} = \omega_0 y_2', \quad (18)$$

$$\ddot{y}_2 = \frac{d^2 y_2}{d\tau^2} = \omega_0^2 \frac{d^2 y_2}{dt^2} = \omega_0^2 y_2'', \quad (19)$$

where the time derivative with respect to the dimensionless time is indicated by a prime ('). Rewriting Eq. (14) in the dimensionless time yields

$$y_2'' + \frac{c}{\omega_0 m} y_2' + y_2 = \underbrace{-\frac{F_{11}}{m_1 \omega_0^2} \sin\left(\frac{\Omega_{11}}{\omega_0} t + \beta_{11}\right)}_{\text{Negligible}} - \frac{F_{12}}{m_1 \omega_0^2} \sin\left(\frac{\Omega_{12}}{\omega_0} t + \beta_{12}\right). \quad (20)$$

Given that Ω_{11} is chosen to be in the nearby of $\Omega_{01} = 1$, the effect of the first term on y_2 is negligibly small. Defining the following parameters

$$\beta := \frac{c}{\omega_0 m}, \quad \varepsilon := \frac{F_{12}}{m_1 \omega_0^2}, \quad \omega := \frac{\Omega_{12}}{\omega_0}, \quad (21)$$

we can rewrite Eq. (20) can be rewritten as follows

$$y_2'' + \beta y_2' + y_2 = -\varepsilon \sin(\omega t + \beta_{12}) \quad \text{if } y_2 > \Delta, \quad (22)$$

$$y_{2+} = y_{2-}, \quad y_{2+}' = -R y_{2-}' \quad \text{if } y_2 = \Delta. \quad (23)$$

Using the so called 'unfolding transformation'

$$y_2 = |z| + \Delta, \quad (24)$$

Eq. (22) can be written as

$$z'' + \beta z' + z = (-\Delta - \varepsilon \sin(\omega t + \beta_{12})) \operatorname{sgn} z \quad \text{if } z \neq 0, \quad (25)$$

$$z_+' - z_-' = -(1 - R) z_-' \quad \text{if } z = 0. \quad (26)$$

Using the Van der Pol transformation with

$$z = A \sin \varphi, \quad z' = A \cos \varphi. \quad (27)$$

and a newly defined, uniformly rotating phase

$$\psi = \omega t + \beta_{12}, \quad (28)$$

Eq. (25) can be transformed to

$$\begin{aligned} A' &= -\beta A \cos^2 \varphi + (-\Delta - \varepsilon \sin \psi) \cos \varphi \operatorname{sgn} \sin \varphi & \text{if } \varphi \neq n\pi, \\ A_+ - A_- &= -(1 - R) A_- & \text{if } \varphi = n\pi, \end{aligned} \quad (29)$$

$$\varphi' = 1 + \beta \sin \varphi \cos \varphi + \frac{\Delta + \varepsilon \sin \psi}{A} |\sin \varphi|, \quad (30)$$

$$\psi' = \omega. \quad (31)$$

With the usual definition of the *resonant surface* and *resonant solutions* as also defined in [31], we focus on the parameter values of ω for which the averaged right hand side becomes discontinuous, as in the vicinity of those values, large amplitude responses may occur. 'Dangerous' terms are

$$\langle \sin \psi \cos \varphi \operatorname{sgn} \sin \varphi \rangle = \frac{1}{2\pi} \int_0^{2\pi} \sin(\omega t + \gamma) \cos t \operatorname{sgn} \sin t dt, \quad (32)$$

$$\langle \sin \psi |\sin \varphi| \rangle = \frac{1}{2\pi} \int_0^{2\pi} \sin(\omega t + \gamma) |\sin t| dt, \quad (33)$$

$$\gamma = \psi_0 - \varphi_0, \quad (34)$$

which expression can have values different from zero for values $\omega_l = 2l$, $l = 1, 2, 3, \dots$. Then, by introducing

$$\delta = \frac{\omega}{2l} - 1, \quad \theta = \varphi - \frac{\psi}{2l}, \quad (35)$$

Eq. (29) can be rewritten as

$$A' = -\beta A \cos^2 \varphi - \Delta \cos(\varphi) \operatorname{sgn}(\sin \varphi) - \varepsilon \sin(2l(\varphi - \theta)) \cos \varphi \operatorname{sgn}(\sin \varphi) \quad \text{if } \varphi \neq n\pi, \quad (36)$$

$$A_+ - A_- = -(1 - R)A_- \quad \text{if } \varphi = n\pi, \quad (37)$$

$$\theta' = -\delta + \beta \sin \varphi \cos \varphi + \frac{\Delta + \varepsilon \sin(2l(\varphi - \theta))}{A} |\sin \varphi|, \quad (38)$$

$$\varphi' = 1 + \beta \sin \varphi \cos \varphi + \frac{\Delta + \varepsilon \sin(2l(\varphi - \theta))}{A} |\sin \varphi|. \quad (39)$$

Taking small values for δ , the discontinuous averaging procedure can be performed. Using the notations of [31], the four integrals to be evaluated are

$$J_1 = \frac{1}{2\pi} \int_0^{2\pi} \sin(2l\varphi) |\sin \varphi| d\varphi = \frac{1}{\pi} \int_0^\pi \sin(2l\varphi) \sin \varphi d\varphi = 0, \quad (40)$$

$$J_2 = \frac{1}{2\pi} \int_0^{2\pi} \cos(2l\varphi) |\sin \varphi| d\varphi = -\frac{2}{\pi(4l^2 - 1)}, \quad (41)$$

$$J_3 = \frac{1}{2\pi} \int_0^{2\pi} \sin(2l\varphi) \cos \varphi \operatorname{sgn} \sin \varphi d\varphi = \frac{4l}{\pi(4l^2 - 1)}, \quad (42)$$

$$J_4 = \frac{1}{2\pi} \int_0^{2\pi} \cos(2l\varphi) \cos \varphi \operatorname{sgn} \sin \varphi d\varphi = 0. \quad (43)$$

Using the above results and averaging yields the following differential equations

$$A' = -\left(\frac{1}{2}\beta + \frac{1-R}{\pi}\right)A - \frac{4l\varepsilon}{\pi(4l^2 - 1)} \cos 2l\theta, \quad (44)$$

$$\theta' = -\delta + \frac{2\Delta}{\pi A} + \frac{2\varepsilon}{\pi(4l^2 - 1)} \frac{\sin(2l\theta)}{A}. \quad (45)$$

Eq. (44) differs from Eq. (3.95) in [31] by the additional factor 3 in the denominator, which is a printing error. Setting the left hand side to 0, the stationary solution, A_* and θ_* can be obtained.

$$\frac{\frac{1}{2}\beta + \frac{1-R}{\pi}}{2l} A_* = -\frac{2\varepsilon}{\pi(4l^2 - 1)} \cos 2l\theta_*, \quad (46)$$

$$\delta A_* - \frac{2\Delta}{\pi} = \frac{2\varepsilon}{\pi(4l^2 - 1)} \sin 2l\theta_*. \quad (47)$$

Eliminating θ_* and introducing

$$\beta_l = \frac{\frac{1}{2}\beta + \frac{1-R}{\pi}}{2l}, \quad \varepsilon_l = \frac{\varepsilon}{4l^2 - 1}, \quad (48)$$

one obtains

$$\beta_l^2 A_*^2 + \left(\delta A_* - \frac{2\Delta}{\pi}\right)^2 = \frac{4\varepsilon_l^2}{\pi^2}. \quad (49)$$

Its solution for A is then

$$A_{1,2} = \frac{2}{\pi} \frac{\delta\Delta \pm \sqrt{\varepsilon_l^2(\beta_l^2 + \delta^2) - \Delta^2\beta_l^2}}{\beta_l^2 + \delta^2}. \quad (50)$$

Only the root with the plus sign is a stable solution (see proof in [31]) therefore the stationary amplitude is

$$A_* = \frac{2}{\pi} \frac{\delta\Delta + \sqrt{\varepsilon_l^2(\beta_l^2 + \delta^2) - \Delta^2\beta_l^2}}{\beta_l^2 + \delta^2}. \quad (51)$$

For fixed Δ , β_l and ε_l but for varying δ the maximal value of A_* can be found by setting

$$\left. \frac{\partial A_*}{\partial \delta} \right|_{\delta_{\max}} \stackrel{!}{=} 0, \quad (52)$$

which leads to

$$\delta_{\max} = \frac{\Delta \beta_l}{\varepsilon_l}. \quad (53)$$

Inserted in Eq. (51) the biggest amplitude value estimated by the analytic approach is

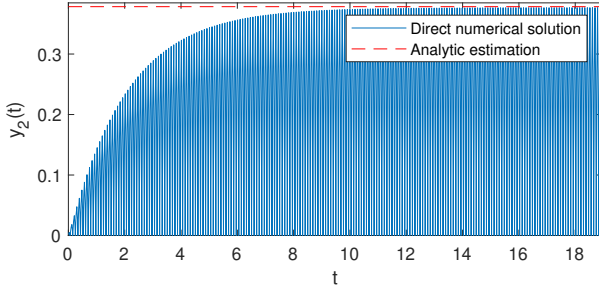
$$A_{*,\max} = \frac{\varepsilon_l}{\beta_l}, \quad (54)$$

independent from Δ , i.e. for every feasible choice of Δ the maximal amplitude is the same for some δ_{\max} . Now we can write the solution

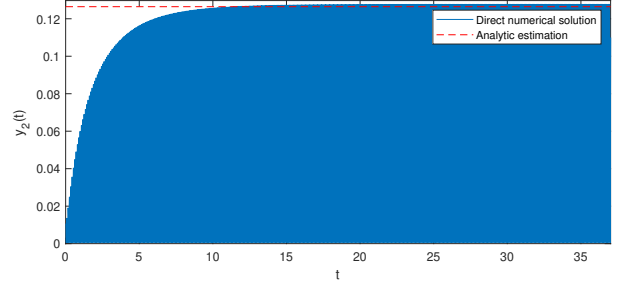
$$z(t) = A_* \sin\left(\frac{\omega t}{2l} + \varphi_0\right) \quad (55)$$

for some φ_0 , thus

$$y_2(t) = A_* \left| \sin\left(\frac{\omega t}{2l} + \varphi_0\right) \right| + \Delta. \quad (56)$$



(a) $m_1 = 1, m_2 = 5, \Omega_{12} = 61.988$ ($l = 1$) and $\Delta = 0$.



(b) $m_1 = 2, m_2 = 1, \Omega_{12} = 138.71$ ($l = 2$) and $\Delta = 0.0006$.

Figure 2: Comparison of the numerical solution for y_2 with the theoretically estimated stationary amplitude for $c = 0.5$, $k = 800$, $F_{12} = 15$. The theoretical model can predict the stationary amplitude very accurately.

The second step of the model reduction: calculating the effective slow potential using the probabilistic description of the high-frequency oscillations

Given the amplitude of y_2 , the PDF of the high-frequency oscillations around the common center of mass, y_1 can be determined as

$$\begin{bmatrix} z_1 \\ z_2 \end{bmatrix} = \begin{bmatrix} x_1 - y_1 \\ x_2 - y_1 \end{bmatrix} = \begin{bmatrix} y_1 - \frac{m_2}{m_1+m_2}y_2 - y_1 \\ y_1 + \frac{m_1}{m_1+m_2}y_2 - y_1 \end{bmatrix} = \begin{bmatrix} -\frac{m_2}{m_1+m_2}y_2 \\ \frac{m_1}{m_1+m_2}y_2 \end{bmatrix}. \quad (57)$$

As it can be expected, the movement is not symmetric around y_1 , unless the masses are equal. In general the PDFs of the individual particles, $\rho_i(x)$ are given by arcsine distributions cut in the middle as depicted in Fig 3. To write the probability density function of z_1 and z_2 , first, we define

$$A_{1*} = (1 - \mu)A_*, \quad A_{2*} = \mu A_*, \quad \Delta_1 = (1 - \mu)\Delta, \quad \Delta_2 = \mu\Delta, \quad (58)$$

thus

$$z_1 = -A_{1*} \left| \sin\left(\frac{\omega t}{2l} + \varphi_0\right) \right| - \Delta_1, \quad z_2 = A_{2*} \left| \sin\left(\frac{\omega t}{2l} + \varphi_0\right) \right| + \Delta_2. \quad (59)$$

In general the probability density function (PDF), $\rho(x)$ of a function, $f(t)$, which is strictly monotonically increasing and continuously differentiable on the interval (a, b) is given by

$$\rho(x) = \frac{1}{f'[f^{-1}(x)]} \cdot \frac{1}{b - a} \quad \text{for } f(a) < x < f(b). \quad (60)$$

If the function, $f(t)$ is strictly monotonically decreasing, its PDF is just the negative of the above expression. Thus in the special case of

$$f(t) = A_{i*} \sin(\Omega t + \beta) + \Delta_i \quad (61)$$

we have

$$\rho(x) = \frac{1}{\Omega \sqrt{A_{i*}^2 - (x - \Delta_i)^2}} \frac{1}{b - a}, \quad (62)$$

where a and b are such, that the function increases monotonically between them. Since $f(t)$ is periodic, it suffices to determine the PDF of one period, which in the case of z_1 and z_2 can be done by splitting the period into a monotonically increasing and monotonically decreasing part. As the two parts obviously has the same PDF in this case, it is enough to determine the PDF of the monotonically decreasing part for z_1 and the monotonically increasing part for z_2 , that we achieve by choosing

$$a = -\frac{2l\varphi_0}{\omega}, \quad b = \frac{2l\left(\frac{\pi}{2} - \varphi_0\right)}{\omega}, \quad \Omega = \frac{\omega}{2l}, \quad (63)$$

then we can write

$$\rho_1(x) = \begin{cases} \frac{2}{\pi \sqrt{A_{1*}^2 - (x + \Delta_1)^2}} & \text{for } -A_{1*} - \Delta_1 < x < -\Delta_1, \\ 0 & \text{otherwise,} \end{cases} \quad (64)$$

$$\rho_2(x) = \begin{cases} \frac{2}{\pi \sqrt{A_{2*}^2 - (x - \Delta_2)^2}} & \text{for } \Delta_2 < x < A_{2*} + \Delta_2. \\ 0 & \text{otherwise.} \end{cases} \quad (65)$$

The PDF of the particle system, $\rho(x)$ is obtained finally by the weighted sum of the individual probability density functions

$$\rho(x) = \mu\rho_1(x) + (1 - \mu)\rho_2(x). \quad (66)$$

A numeric example is given in Fig. 3.

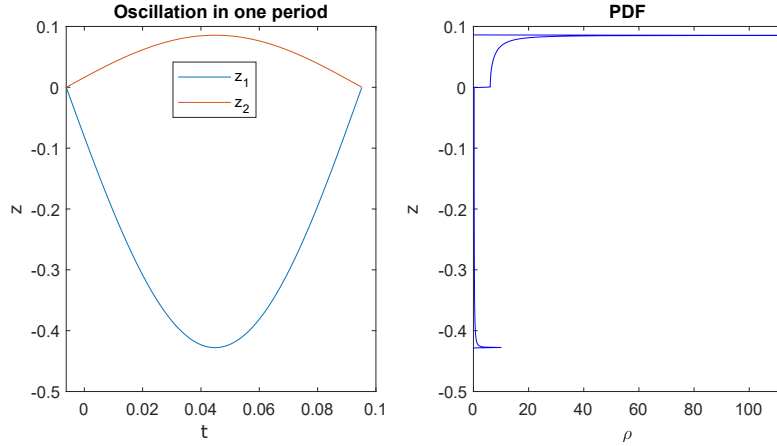


Figure 3: One period of the high-frequency oscillation and the corresponding PDF with masses $m_1 = 1$ and $m_2 = 5$.

Effective potential by convolution

Eq. (9) can be rewritten now as follows

$$\ddot{y}_1 + \mu V'(y_1 + z_1) + (1 - \mu)V'(y_1 + z_2) = \frac{1}{m_1 + m_2} (F_{11} \sin(\Omega_{11}\tau + \beta_{11}) + F_{12} \sin(\Omega_{12}\tau + \beta_{12})). \quad (67)$$

The arguments of $V'(\cdot)$ oscillates with a high frequency around y_1 , instead of calculating the exact values for every moment, a kind of averaging is used to obtain an effective potential \tilde{V} . As during a period of the high frequency vibration z_i the change of y_1 is small, we can get the averaged force at y_1 by calculating the total force on the particle density cloud at y_1 having the PDF $\rho_1(x)$ and $\rho_2(x)$. The latter operation can be performed, as for any continuously distributed volume in a force field, by the following integral transformation

$$\tilde{V}'(y_1) = \int_{-\infty}^{\infty} V'(x)\rho(x - y_1)dx. \quad (68)$$

In our special case the integral can be evaluated analytically. First we define the positions

$$d_1 = -1 - \Delta_2 - A_{2*}, \quad d_2 = -1 - \Delta_2, \quad d_3 = -1 + \Delta_1, \quad d_4 = -1 + \Delta_1 + A_{1*}, \quad (69)$$

$$d_5 = 1 - \Delta_2 - A_{2*}, \quad d_6 = 1 - \Delta_2, \quad d_7 = 1 + \Delta_1, \quad d_8 = 1 + \Delta_1 + A_{1*}. \quad (70)$$

In the following, we will only consider the case, when $\Delta + A_* < 2$, so that we can guarantee that $d_1 \dots d_9$ are in ascending order. With the help of the above positions we can define the domains

$$D_1 = \{x \in \mathbb{R} | x \leq d_1\}, \quad (71)$$

$$D_i = \{x \in \mathbb{R} | d_{i-1} \leq x < d_i\} \quad \text{for } i = 2 \dots 8, \quad (72)$$

$$D_9 = \{x \in \mathbb{R} | d_8 \leq x\}. \quad (73)$$

Thus, the effective force field can be written as

$$\tilde{V}'(y_1) = \begin{cases} 0 & x \in D_1, \\ (1 - \mu) \left(y_1 + \Delta_2 + \frac{2}{\pi} \left(\sqrt{A_{2*}^2 - (1 + \Delta_2 + y_1)^2} - (y_1 + \Delta_2) \arcsin \left(-\frac{1 + \Delta_2 + y_1}{A_{2*}} \right) \right) \right) & x \in D_2, \\ (1 - \mu) \left(y_1 + \Delta_2 + \frac{2}{\pi} A_{2*} \right) & x \in D_3, \\ \mu \left(\frac{2}{\pi} \left(\sqrt{A_{1*}^2 - (\Delta_1 - 1 - y_1)^2} + (\Delta_1 - y_1) \arcsin \left(\frac{\Delta_1 - 1 - y_1}{A_{1*}} \right) - A_{1*} \right) \right) + (1 - \mu) \left(y_1 + \Delta_2 + \frac{2}{\pi} A_{2*} \right) & x \in D_4, \\ y_1 & x \in D_5, \\ \mu \left(y_1 - \Delta_1 - \frac{2}{\pi} A_{1*} \right) + (1 - \mu) \left(\frac{2}{\pi} \left(A_{2*} - \sqrt{A_{2*}^2 - (1 - \Delta_2 - y_1)^2} + (\Delta_2 + y_1) \arcsin \left(\frac{1 - \Delta_2 - y_1}{A_{2*}} \right) \right) \right) & x \in D_6, \\ \mu \left(y_1 - \Delta_1 - \frac{2}{\pi} A_{1*} \right) & x \in D_7, \\ \mu \left(-\frac{2}{\pi} \left(\sqrt{A_{1*}^2 - (1 + \Delta_1 - y_1)^2} + (\Delta_1 - y_1) \arcsin \left(\frac{1 + \Delta_1 - y_1}{A_{1*}} \right) \right) - \Delta_1 + y_1 \right) & x \in D_8, \\ 0 & x \in D_9. \end{cases} \quad (74)$$

Through integration the effective potential can be determined as well. As the potential can be shifted arbitrarily by a constant, we set the condition $\tilde{V}(-\infty) \stackrel{!}{=} 0$. However, the analytic expression for $\tilde{V}(y_1)$ is very complex, so we dispense with giving an exact formula here.

Please note, that Eq. (74) is valid for arbitrary values of Δ , however, in practical cases Δ is limited to $\mathcal{O}(\varepsilon)$, thus the intervals D_3 and D_7 do not have a significant role.

In Fig. 4 a graphical example is represented for a certain parameter choice (cf. the caption of Fig. 4).

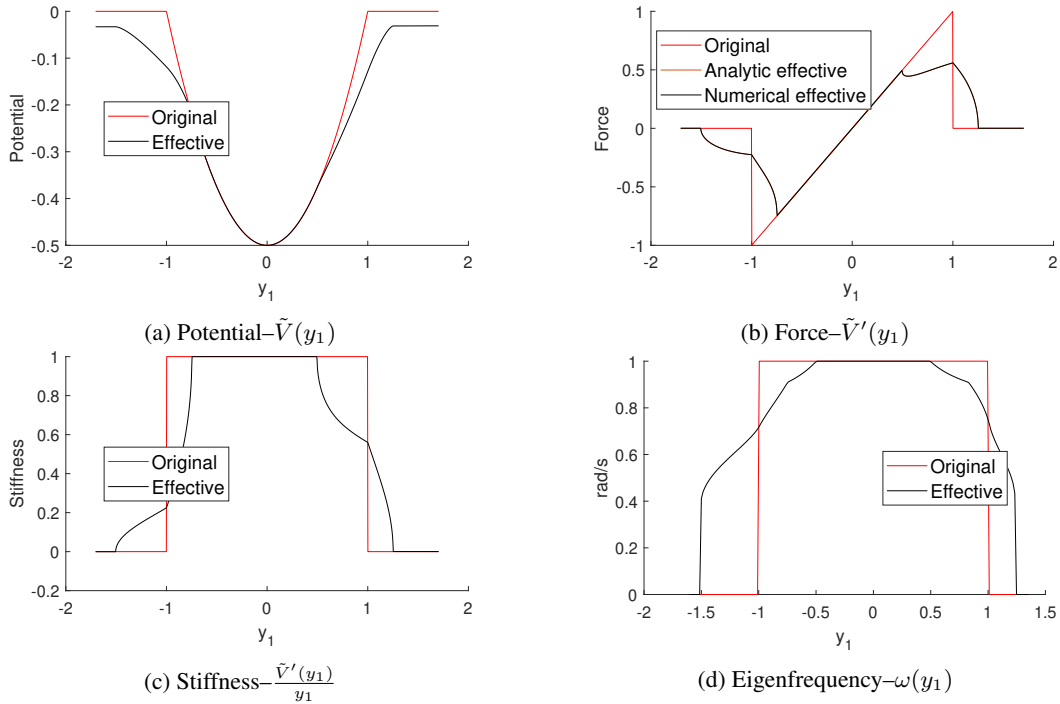
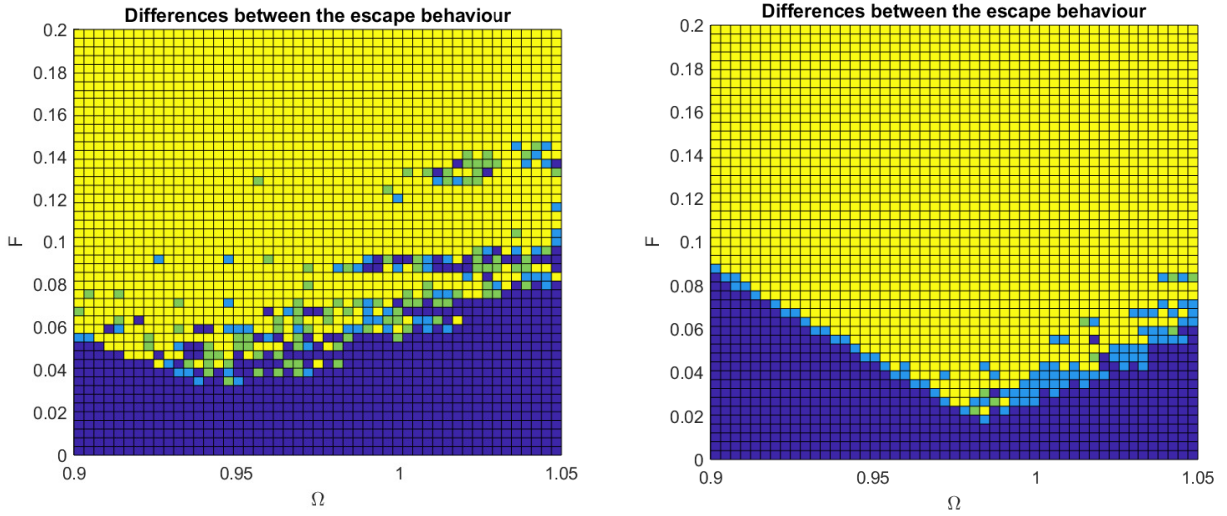


Figure 4: Non-linear force field and some other derived quantities generated by $m_1 = 2$, $m_2 = 1$, $c = 0.5$, $k = 800$, $F_{12} = 30$, $\Omega_{12} = 69.335$ ($l = 1$), $\Delta = 0.0006$.

A very important effect, due to the asymmetric integration kernel, is the asymmetry of the effective force field. Therefore all the other quantities derived from it, are asymmetric as well. Moreover, the potential energy on the right boundary of the potential is also different from the potential energy on the left hand side of the potential, which might lead to an asymmetric escape behavior. The probabilities of escaping to the right might differ from the probability of escaping to the left. The further the ratio $\frac{m_1}{m_2}$ is from 1, the greater is the asymmetry, which leads to vibrations with a symmetry center different from 0.

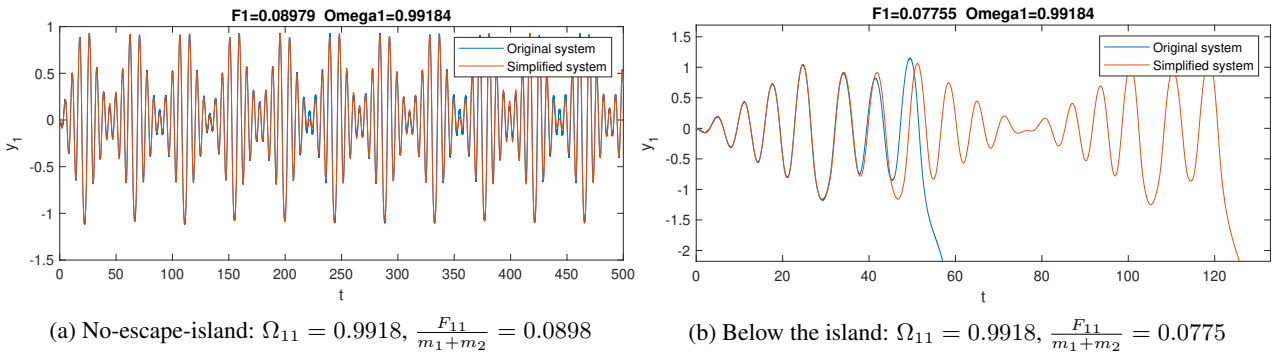
Numerical results and discussion

A good way to determine the goodness of the order reduction method applied above is to depict the escaping/non-escaping points on the low excitation frequency–low excitation force plane. In Fig. 5 such a comparison can be seen. It is important to note, that the sharp minimum (Ω_C, F_C), observed by many authors in the literature, can be determined more or less. However, in Fig. 5 on the right from the minimum, i.e. for $\Omega_{11} > \Omega_C$ there is not really a frequency dependent critical forcing value, above which escape happens for whatever forcing amplitude. Instead the transition from no-escape into escape happens through a fractal-like boundary and there exist even separated non-escaping 'islands' in the 'see' of escaping $\Omega_{11} - F_{11}$ parameter combinations. Such a time evolution is shown in Fig. 6. The remarkable feature of the model reduction is, that even these non-escaping islands of the parameter combinations remain preserved. When the non-linear part of the effective force gets smaller (cf. 5b), we can observe a less chaotic behavior around the critical force values. Moreover, it is also obvious that the minimally needed force amplitude moves up, as the non-linearity of the effective force field increases, due to the increasing amplitude of the relative motion. This simple fact explains also, why the escaping region in the $\Omega_{11} - F_{11}$ plane moves closer to the point (1, 0), when the relative motion is excited with a higher resonant frequency but unchanged force amplitude. Eq. (54) and Eq. (48) show the simple relationship between the excitation frequency and the amplitude of the caused resonant motion that shows a decreasing amplitude with increasing value for l .



(a) First resonant frequency is excited, $\Omega_{12} = 69.34$ ($l = 1$). (b) Second resonant frequency is excited, $\Omega_{12} = 138.67$ ($l = 2$).

Figure 5: Comparison of the reduced model to the original one with parameter values $m_1 = 2, m_2 = 1, c = 0.5, k = 800, F_{12} = 30$, and $\Delta = 0.0006$. Dark blue dots mean no escape for both models, bright blue is escape in the simplified model, but no escape in the original model, green is no escape in the simplified model, but escape in the original one. Yellow stands for escape in both models. $F := \frac{F_{11}}{m_1 + m_2}$.



(a) No-escape-island: $\Omega_{11} = 0.9918, \frac{F_{11}}{m_1 + m_2} = 0.0898$

(b) Below the island: $\Omega_{11} = 0.9918, \frac{F_{11}}{m_1 + m_2} = 0.0775$

Figure 6: $m_1 = 2, m_2 = 1, c = 0.5, k = 800, F_{12} = 30, \Omega_{12} = 69.335$ ($l = 1$) and $\Delta = 0.0006$.

Conclusions

In the present work escape of a strongly coupled, colliding pair of particles from a potential well under bi-harmonic excitation was investigated. Through a coordinate transformation from the physical coordinates of the particles into the coordinates of the common center of mass and into the distance of the particles the motion could be decomposed into a

slow and into a fast variable. After determining the oscillation amplitudes of the fast motion with the use of the so called 'unfolding transformation', a certain type of averaging, appropriate to use also with piece-wisely defined functions being based on the probability density function of the fast motion, was performed. The resulting formulas for the effective force-field are fully analytic, thus a huge reduction in the simulation time can be achieved (5 hours vs 4 minutes in the example shown). It turns out, that even such properties of the system remain well conserved, as for example the location of the non-escaping islands on the low excitation frequency–low forcing amplitude ($\Omega_{11} - F_{11}$) plane. Although in the current work escape was investigated in a truncated quadratic potential well, the application of the PDF based averaging method is straightforward for several different potentials as well.

Many questions may remain open in the Reader regarding the further analysis of the escape behavior of a colliding pair of coupled particles. What happens if the resonant frequencies of the relative motion are of the same magnitude as the eigenfrequency of the bottom of the potential well? How do the initial conditions of the particles influence the escape behavior? How to proceed in case of poly-harmonic excitation? What if the collision of the particles is a random process? What happens when there are more than two colliding particles?

The authors of this paper hope, that many of the readers will feel motivated to find answers to these and many other different questions arising when studying the thrilling topic of escape from a potential well.

References

- [1] Landau, L.D., Lifshitz, E.M.: *Mechanics*, 3rd edn. Butterworth, Herrmann (1976)
- [2] Thompson, J.M.T.: Chaotic phenomena triggering the escape from a potential well. In: Szemplinska-Stupnicka, W., Troger, H. (eds.) *Engineering Applications of Dynamics of Chaos*, CISM Courses and Lectures, vol. 139, pp. 279–309. Springer, Brelin (1991)
- [3] Lawrence N. Virgin, Raymond H. Plaut, Ching-Chuan Cheng, Prediction of escape from a potential well under harmonic excitation, *International Journal of Non-Linear Mechanics*, Volume 27, Issue 3, 1992, Pages 357-365, ISSN 0020-7462, [https://doi.org/10.1016/0020-7462\(92\)90005-R](https://doi.org/10.1016/0020-7462(92)90005-R).
- [4] Virgin, L.N.: Approximate criterion for capsizes based on deterministic dynamics. *Dyn. Stab. Syst.* 4, 56–70 (1989)
- [5] Sanjuan, M.A.F.: The effect of nonlinear damping on the universal escape oscillator. *Int. J. Bifurc. Chaos* 9, 735–744 (1999)
- [6] Mann, B.P.: Energy criterion for potential well escapes in a bistable magnetic pendulum. *J. Sound Vib.* 323, 864–876 (2009)
- [7] Barone, A., Paterno, G.: *Physics and Applications of the Josephson Effect*. Wiley, New York (1982)
- [8] Arnold, V.I., Kozlov, V.V., Neishtadt, A.I.: *Mathematical Aspects of Classical and Celestial Mechanics*. Springer, Berlin (2006)
- [9] Quinn, D.D.: Transition to escape in a system of coupled oscillators. *Int. J. Non-Linear Mech.* 32, 1193–1206 (1997)
- [10] Belenky, V.L., Sevastianov, N.B.: *Stability and Safety of Ships—Risk of Capsizing*. The Society of Naval Architects and Marine Engineers, Jersey City (2007)
- [11] Elata, D., Bamberger, H.: On the Dynamic Pull-In of Electrostatic Actuators with Multiple Degrees of Freedom and Multiple Voltage Sources. *Journal of Microelectromechanical Systems* 15, 131–140 (2006)
- [12] Leus, V., Elata, D.: On the dynamic response of electrostatic MEMS switches. *J. Microelectromech. Syst.* 17, 236–243 (2008)
- [13] Younis, M.I., Abdel-Rahman, E.M., Nayfeh, A.: A reduced-order model for electrically actuated microbeam-based MEMS. *J. Microelectromech. Syst.* 12, 672–680 (2003)
- [14] Alsaleem, F.M., Younis, M.I., Ruzziconi, L.: An experimental and theoretical investigation of dynamic pull-in in MEMS resonators actuated electrostatically. *J. Microelectromech. Syst.* 19, 794–806 (2010)
- [15] Ruzziconi, L., Younis, M.I., Lenci, S.: An electrically actuated imperfect microbeam: dynamical integrity for interpreting and predicting the device response. *Meccanica* 48, 1761–1775 (2013)
- [16] Zhang, W.-M., Yan, H., Peng, Z.-K., Meng, G.: Electrostatic pull-in instability in MEMS/NEMS: a review. *Sens. Actuators A Phys.* 214, 187–218 (2014)
- [17] Kramers, H.A.: Brownian motion in a field of force and the diffusion model of chemical reactions. *Physica (Utrecht)* 7, 284–304 (1940)
- [18] Fleming, G.R., Hanggi, P.: *Activated Barrier Crossing*. World Scientific, Singapore (1993)
- [19] Talkner, P., Hanggi, P. (eds.): *New Trends in Kramers' Reaction Rate Theory*. Springer, Berlin (1995)
- [20] Rega, G., Lenci, S.: Dynamical integrity and control of nonlinear mechanical oscillators. *J. Vib. Control* 14, 159–179 (2008)
- [21] Diego Orlando, Paulo B. Gonçalves, Stefano Lenci, Giuseppe Rega, Influence of the mechanics of escape on the instability of von Mises truss and its control, *Procedia Engineering*, Volume 199, 2017, Pages 778-783, ISSN 1877-7058, <https://doi.org/10.1016/j.proeng.2017.09.048>.
- [22] Gendelman, O.V. Escape of a harmonically forced particle from an infinite-range potential well: a transient resonance. *Nonlinear Dyn* 93, 79–88 (2018). <https://doi.org/10.1007/s11071-017-3801-x>
- [23] Manevitch, L.I.: New approach to beating phenomenon in coupled nonlinear oscillatory chains. *Arch. Appl. Mech.* 77, 301–312 (2007)
- [24] Manevitch, L.I., Gendelman, O.V.: *Tractable Modes in Solid Mechanics*. Springer, Berlin (2011)
- [25] Gendelman, O.V., Karmi, G. Basic mechanisms of escape of a harmonically forced classical particle from a potential well. *Nonlinear Dyn* 98, 2775–2792 (2019). <https://doi.org/10.1007/s11071-019-04985-9>
- [26] V.M. Volosov, B.I. Morgunov, *Method of Averaging in the Theory of nonlinear Oscillating Systems*, Moscow State University, Moscow, 1971 (in Russian).
- [27] M Balachandra, PR Sethna, A generalization of the method of averaging for systems with two time scales. *Archive for Rational Mechanics and Analysis*, 1975 – Springer, <https://link.springer.com/content/pdf/10.1007/BF00280744.pdf>
- [28] Genda, A., Fidin, A. & Gendelman, O. On the escape of a resonantly excited couple of particles from a potential well. *Nonlinear Dyn* (2021). <https://doi.org/10.1007/s11071-021-06312-7>
- [29] Alexander Fidin, Olga Drozdetskaya, On the Averaging in Strongly Damped Systems: The General Approach and its Application to Asymptotic Analysis of the Sommerfeld Effect, *Procedia IUTAM*, Volume 19, 2016, Pages 43-52, ISSN 2210-9838, <https://doi.org/10.1016/j.piutam.2016.03.008>.
- [30] Fidin A, Thomsen J.J. Non-trivial effects of high-frequency excitation for strongly damped mechanical systems. *Int. J. of Non-Linear Mechanics* 2008; 43: 569 – 578.
- [31] A. Fidin, *Nonlinear Oscillations in Mechanical Engineering*, 1st edn. Springer-Verlag Berlin Heidelberg, 2006, ISBN 978-3-540-28116-0, DOI 10.1007/3-540-28116-9
- [32] Guckenheimer, J. and Holmes, P. 1983 *Nonlinear oscillations, dynamical systems, and bifurcations of vector fields*. New York: Springer-Verlag.